High-accuracy frequency standards using laser-cooled Hg$^+$ ions*

D.J. Berkeland, J.D. Miller, B.C. Young, J.C. Bergquist, W.M. Itano, and D.J. Wineland

National Institute of Standards and Technology, Time and Frequency Division

Boulder, CO 80303

Abstract

We discuss frequency standards based on laser-cooled ^{199}Hg$^+$ ions confined in cryogenic rf (Paul) traps. In one experiment, the frequency of a microwave source is servoed to the ions' ground-state hyperfine transition at 40.5 GHz. For seven ions and a Ramsey free precession time of 100 s, the fractional frequency stability is $3.3\,(2) \times 10^{-13}\,\tau^{-1/2}$ for measurement times $\tau < 2$ h. The ground-state hyperfine interval is measured to be 40 507 347 996.841 59 (14) (41) Hz, where the first number in parentheses is the uncertainty due to statistics and systematic errors, and the second is the uncertainty in the frequency of the time scale to which the standard is compared. In a second experiment under development, a strong-binding cryogenic trap will confine a single ion used for an optical frequency standard based on a narrow electric quadrupole transition at 282 nm. The bandwidth of the laser used to drive this transition is less than 10 Hz at 563 nm.

Keywords: trapped atoms, ion trap, laser cooling, frequency standards, hyperfine structure, stabilized lasers

1. Introduction

Trapped and cooled ions can be used for sensitive measurements which, for several reasons, are frequently not feasible using typical thermal atomic sources. First, it is possible to measure and to manipulate the quantum states of individual ions. This allows measurements of quantum mechanical effects such as quantum jumps [1] and preparation of the atoms' internal states toward, for example, spin squeezing [2]. Also, individual ions can be observed for very long times, so that narrow atomic transitions can be detected with extremely high resolution. Finally, the well-controlled environment of the ion trap can significantly reduce systematic effects such as Stark and Zeeman shifts. All of these factors make trapped, cold ions excellent candidates for frequency standards. Stable and accurate atomic frequency standards [3] are not only useful for measuring time, but are often the realization of other basic units, are necessary in navigation and communication, and are frequently used in investigations of physical phenomena [4].

At NIST, our goal is to develop frequency standards that achieve high accuracy in addition to high stability. We confine strings of laser-cooled ^{199}Hg$^+$ ions in a linear rf trap such as that depicted in Fig. 1 [5]. A linear trap can confine many laser-cooled ions along the rf nodal line. Here, the atomic motion driven by the oscillating electric field of the trap (the micromotion) vanishes, so Doppler shifts and ac Stark shifts are negligible [6, 7]. Furthermore, the increase in the kinetic energy of the ions caused by the electric field is minimized, so perturbative cooling laser radiation can be removed during the long probe periods of the clock transition. We trap and cool ^{199}Hg$^+$, which offers a microwave clock transition at 40.5 GHz and an optical clock transition at 1.06×10^{15} Hz (see Fig. 2). To first-order, both transitions are insensitive to magnetic and electric fields at zero fields. Using linear crystals of ^{199}Hg$^+$ ions, we expect to reduce all systematic frequency shifts to less than a part in 10^{16}.

A trapped ion frequency standard can also have high statistical precision. If the fluctuations of the atomic signal are due only to quantum statistics, then the stability of a frequency source servoed to the atomic transition is given by [8, 9]

$$\sigma_y(\tau) = \frac{1}{\omega_0 \sqrt{N\,T_R}}\,\tau^{-1/2}, \tag{1}$$

where ω_0 is the frequency of the atomic transition, N is the number of ions, T_R is the Ramsey interrogation time, and τ is the averaging time of the measurement. For the ground-state hyperfine transition, $\omega_0/2\pi = 40.5$ GHz. It appears feasible to use $N = 100$ ions and $T_R = 100$ s, which gives $\sigma_y(\tau) \approx 4 \times 10^{-14}\,\tau^{-1/2}$. For the 282 nm $5d^{10}6s\,^2S_{1/2} \rightarrow 5d^96s^2\,^2D_{5/2}$ electric quadrupole transition, $\omega_0/2\pi = 10^{15}$ Hz, so that using $N = 1$ and $T_R = 25$ ms gives $\sigma_y(\tau) \approx 10^{-15}\,\tau^{-1/2}$.

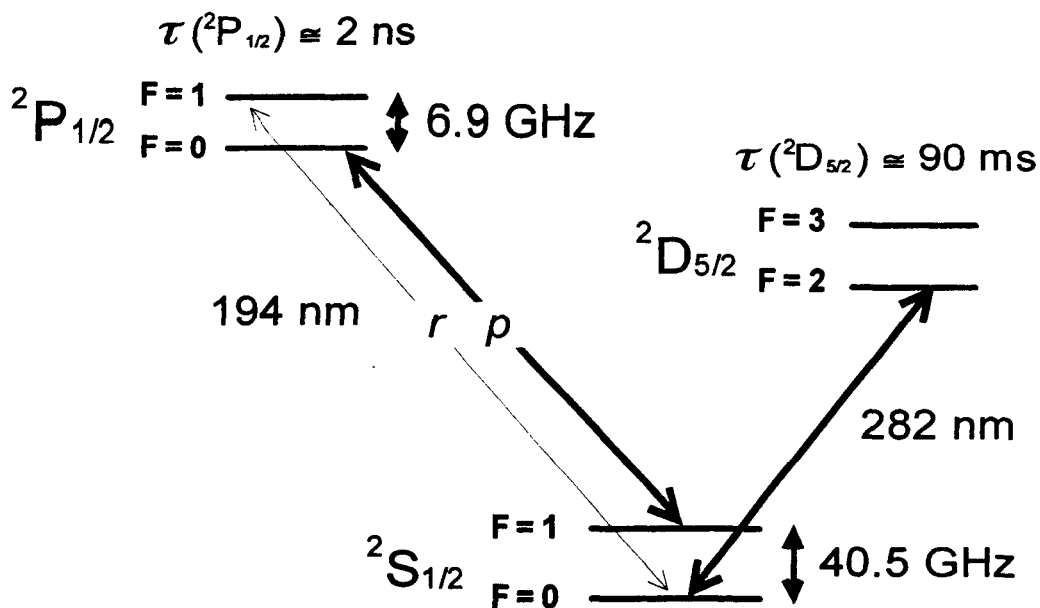$$\tau\,(^2P_{1/2}) \cong 2 \text{ ns}$$

Figure 1: Partial energy diagram of $^{199}\text{Hg}^+$. The 70 MHz wide 194 nm transitions are used for laser cooling and detection. The 40.5 GHz and 282 nm transitions are the clock transitions.

We discuss the evaluation of a clock based on the 40.5 GHz ground-state hyperfine transition in $^{199}\text{Hg}^+$. We also discuss the development of a frequency standard based on the 282 nm electric quadrupole transition, and the narrow band source of 563 nm radiation needed to drive this transition.

2. Cryogenic Linear rf Trap

Figure 2 shows the linear rf trap used in the 40.5 GHz microwave frequency standard. Two diagonally opposite rods are grounded, while the potential of the other two rods is $V_0 \cos(\Omega\, t)$, where $V_0 \approx 150$ V and $\Omega/2\pi = 8.6$ MHz. The resulting pseudopotential confines the ions radially in a well with a secular frequency $\omega_r/2\pi \approx 230$ kHz. To remove patch fields and electrical charge that otherwise leave the rods only slowly in the cryogenic environment, we thread insulated wires through the rods to heat them. Two cylindrical sections at either end of the trap are held at a potential of approximately +10 V, confining the ions in an axial potential well of secular frequency of $\omega_z/2\pi \approx 15$ kHz. The ions are laser-cooled using the 194 nm, $5d^{10}6s\ ^2S_{1/2} \rightarrow 5d^{10}6p\ ^2P_{1/2}$ electric dipole transitions shown in Fig. 2. Typically, a string of approximately ten ions is confined near the trap axis. By minimizing the ion micromotion in all three dimensions, we assure that the laser-cooled ions lie along the rf nodal line [10].

We place the trap in a cryogenic environment to reduce two problems associated with background gas. We previously used a linear rf trap at room temperature with a background pressure of approximately 10^{-8} Pa [11]. At this pressure, background neutral Hg atoms cause Hg^+ loss, presumably by forming dimers with ions excited by the cooling laser. This limited the ion storage time to about ten minutes. At liquid He temperatures, however, Hg and most other background gases are cryopumped onto the walls of the chamber, allowing us to confine laser-cooled Hg^+ ions without loss for periods of over ten hours. Even in the absence of laser cooling during overnight down periods, we have confined strings of approximately ten ions for several days. In addition, at this low background pressure, pressure shifts should be negligible.

Operation at 4 K also reduces the frequency shifts due to blackbody radiation of the $^{199}\text{Hg}^+$ ground-state hyperfine transition. At $T = 4$ K, the fractional blackbody Zeeman shift is -2×10^{-21}, and the fractional blackbody Stark shift is -3×10^{-24} [12]. This is significantly smaller than the fractional blackbody Stark shift for neutral Cs ($1.69(4) \times 10^{-14}$ at $T = 300$ K [12]).
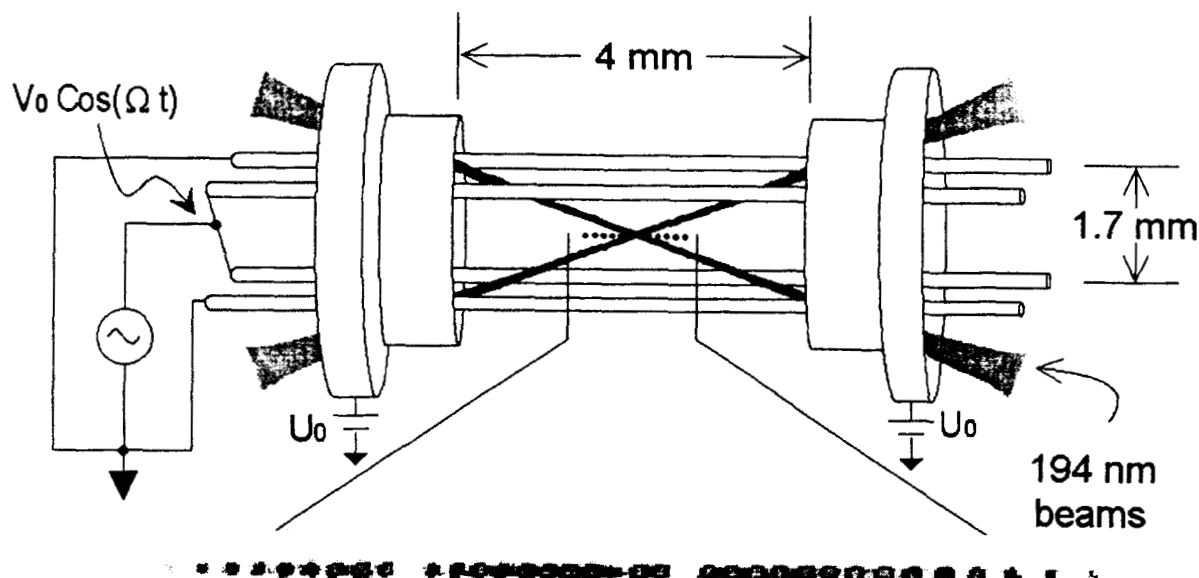
Figure 2: Linear rf trap, and an image of a linear ion crystal. The ions are spaced approximately 10 μm apart, and apparent gaps in the ion crystal are due to ions other than ^{199}Hg$^+$, which do not fluoresce at the frequencies of the 194 nm laser beams. The spatial extent of the ions is exaggerated for clarity; in reality the laser beams overlap all the ions.

3. Laser-atom Interactions

Laser beams at 194 nm [13] are used both for cooling and for determining the internal states of the ions. To cool the ions, we tune the frequency of a primary laser slightly below resonance with transition p. Although this is nearly a cycling transition (see Fig. 2), the laser can off-resonantly excite an ion into the $^2P_{1/2}$, $F = 1$ level, from which the ion can decay into the $^2S_{1/2}$, $F = 0$ level. To maintain fluorescence, a repumping laser beam, resonant with transition r, is overlapped collinearly with the primary laser beam.

To determine the atomic state, the primary beam is pulsed on for a time comparable to the time necessary to pump the ions from the $^2S_{1/2}$, $F = 1$ to the $^2S_{1/2}$, $F = 0$ level (typically 10 ms). If the ion is found in the $^2S_{1/2}$, $F = 1$ level, it will scatter about 10^4 photons before it optically pumps into the $^2S_{1/2}$, $F = 0$ level. We detect and count approximately 150 of these photons. If the transition is not saturated, the number of photons scattered before the ion is optically pumped can be made nearly insensitive to laser power. If the ion is found in the $^2S_{1/2}$, $F = 0$ level, it will scatter only a few photons, so the atomic state can be determined with certainty if the ions are monitored individually. Thus, the signal-to-noise ratio of the state detection signal can be limited only by the quantum uncertainty in the atomic state [9]. Currently, however, the state-detection signal is simply the combined fluorescence from all the ions. As a result, we think that fluctuations in the frequency of the 194 nm light and its intensity at the site of the ions limit our typical stability to about twice that of Eq. (1).

Laser cooling and state detection are further complicated by the ^{199}Hg$^+$ ground-state hyperfine structure. If the laser polarization is constant and the magnetic field is zero, two superpositions of the $^2S_{1/2}$, $F = 1$, magnetic sublevels are dark states. An ion optically pumps into these dark states after scattering only a few photons, after which the fluorescence vanishes. To constantly pump the ions out of the dark states, the laser field must couple each $^2S_{1/2}$, $F = 1$, magnetic sublevel to the $^2P_{1/2}$, $F = 0$ level, and each of these three couplings must have a different time dependence. These conditions can be achieved only by using two non-collinear laser beams. We continuously cycle the polarization state of one laser beam between left and right circular polarizations. The linear polarization of the second beam remains fixed in the plane formed by the two beams, which overlap with the ions at a 40° angle to each other.

4. The 40.5 GHz Microwave Clock

For the first part of our measurement cycle, we cool the ions by pulsing on both the primary and repumping 194 nm laser beams for 300 ms. Next, we turn off the repumping beam for about 90 ms, so that essentially all of the ions are optically pumped into the $^2S_{1/2}$, $F = 0$ level. We probe the clock transition using the Ramsey technique of separated oscillatory fields [14]. Both beams are blocked during the Ramsey microwave interrogation period, which consists of two 250 ms microwave pulses separated by the free precession period T_R. We vary T_R from 2 to 100 s, which is useful in searching for possible systematic frequency shifts, as explained below. Finally, we turn on the primary beam for about 10 ms while counting the number of detected photons. This determines the ensemble average of the atomic state population and completes one measurement cycle.

We derive the microwave frequency from a low-noise crystal quartz oscillator locked to a reference hydrogen maser [15]. To steer the average microwave frequency into resonance with the clock transition, we step the frequency by $+\Delta f$, then $-\Delta f$, about frequency f_M ($\cong \omega_0/2\pi$), and complete a measurement cycle after each step. Usually, the output frequencies lie near the half-maximum points of the central Ramsey fringe. On successive measurement pairs, we alternate the signs of the frequency steps to avoid any systematic frequency shift due to a linear drift in, for example, the signal size or background counts. The error signal ε_M is the difference between the number of detected photons for the pair of measurement cycles. Finally, a digital servo adjusts the average frequency according to

$$f_{M+1} = f_0 + g_p \varepsilon_M + g_i \sum_{m=1}^{M} \varepsilon_m , \qquad (2)$$

where f_0 is the initial value of the frequency, and the proportional gain g_p and the integral gain g_i are set independently of each other. Typically, the maximum value of M for a single run is about 130. The average frequency for each run is calculated after discarding the first four recorded frequencies f_i, to remove offsets caused by a mismatch between the initial frequency f_0 and the clock transition frequency.

Figure 3 shows the fractional frequency stability $\sigma_y(\tau)$ of the steered microwave frequency for seven ions and Ramsey times of 10 s and 100 s. When $N = 7$ and $T_R = 100$ s is $\sigma_y(\tau) \cong 3.3$ (2) $\times 10^{-13} \ \tau^{-1/2}$, for $\tau \leq 2$ h. For all parameters, the measured $\sigma_y(\tau)$ is about twice the value expected from Eq. (1), primarily because of laser intensity fluctuations at the site of the ions. Our measured frequency stability is comparable to those of the Cs beam standard
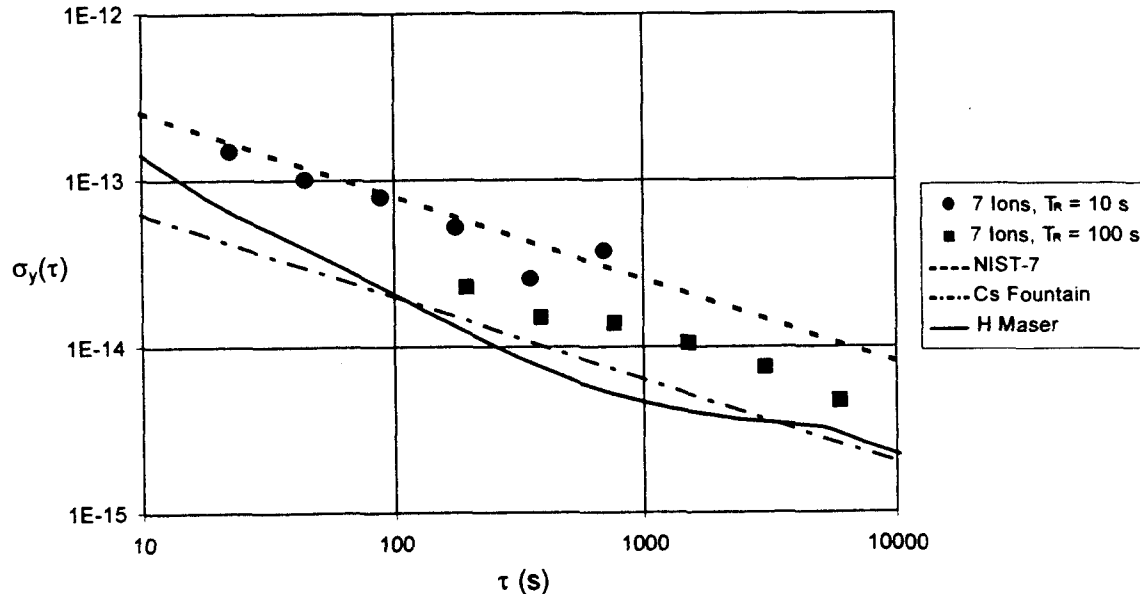

Figure 3: Stability plots for the 40.5 GHz microwave clock, using $N = 7$ ions, and both $T_R = 10$ s and $T_R = 100$ s. Also shown is the stability of the Cs beam standard NIST-7 [16], of the Cs fountain standard [17], and of the hydrogen maser.

Table 1: Systematic shifts of the average clock transition frequency. Typical values are for an rf power delivered to the trap of $P_{rf} = 20$ mW, a Ramsey interogation time of $T_R = 100$ s, and a static magnetic field of $B_{static} = 3 \times 10^{-7}$ T. Here, B_Ω is the magnetic field component at frequency Ω, I_p is the intensity of the scattered primary beam during the Ramsey interrogation time, δ_p the detuning of the frequency of the primary beam from that of transition p, and γ the linewidth of the cooling transitions.

Shift	Scaling	Magnitude of Effect (Typical)	Uncertainty in Effect
Quadratic Zeeman (static)	$+ <B_{static}^2>$	2×10^{-14}	1.4×10^{-15}
Quadratic Zeeman (Ω)	$+ <B_\Omega^2>$	5×10^{-15}	3.2×10^{-15}
Microwave chirp, leakage, and spectrum asymmetries	$1/T_R$	3×10^{-15}	8×10^{-16}
Light shift from 194 nm	$\dfrac{I_p \delta_p}{\delta_p^2 + \gamma^2}$	$< 3 \times 10^{-16}$	$< 3 \times 10^{-16}$

NIST-7, for which $\sigma_y(\tau) \cong 8 \times 10^{-13} \tau^{-1/2}$ [16], and the Cs fountain standard, for which $\sigma_y(\tau) \cong 2 \times 10^{-13} \tau^{-1/2}$ [17].

Table 1 shows the most important corrections we make to the average frequency for each run [18]. The fractional Zeeman shift due to the static magnetic field is $+0.24 B_{static}^2$, where B_{static} is expressed in teslas. By measuring the Zeeman splitting of the ground state hyperfine transitions, we find that the peak-to-peak variation in the static magnetic field between the beginning and end of a run is at most 1×10^{-8} T. Since, typically, $B_{static} \cong 3 \times 10^{-7}$ T, an upper bound on the fractional uncertainty in this Zeeman shift is 1.4×10^{-15}.

We also correct for an ac Zeeman shift that depends linearly on the rf power P_{rf} delivered to the trap. The uncertainty in this correction dominates the overall uncertainty of the clock transition frequency. This shift is caused by magnetic fields due to currents at frequency Ω in the trap electrodes, which are not present in an ideal trap. Since these currents are not necessarily symmetric with respect to the trap nodal line, the magnetic fields they produce do not cancel at the site of the ions. Considering that the distribution of these currents may vary from load to load, we measure the average transition frequency for P_{rf} ranging from about 17 mW ($V_0 \cong 140$ V) to 68 mW ($V_0 \cong 270$ V) for each ion crystal. A fit to these data gives the frequency shift $(d\omega/dP_{rf})/\omega_0$ and the extrapolated frequency at zero rf power ω_0, for that crystal. Typically, $(d\omega/dP_{rf})/\omega_0 \cong (2.5 \pm 2.1) \times 10^{-16}$ /mW; within the uncertainty, this value is the same for each crystal. The uncertainty in the extrapolated frequency averaged over five ion crystals used in the frequency measurement is 3.2×10^{-15}.

The magnitudes of several frequency shifts scale with the free precession time as $1/T_R$. These include shifts due to the phase chirp of the microwaves as they are switched on and off, any leakage microwave field present during the free precession time T_R, and asymmetries in the microwave spectrum. By varying T_R, we measure the fractional shift from these combined effects to be $-3 (3) \times 10^{-14} /T_R$ (where T_R is in seconds). Finally, we measured the intensity of the scattered 194 nm light at the site of the ions when the 194 nm sources are blocked. This determines the ac Stark shift due to stray 194 nm light present during the Ramsey interrogation time to be $< 3 \times 10^{-16}$.

The fits to the transition frequencies as a function of rf power give the extrapolated frequency ω_0 at zero rf power. Figure 4 shows the variation in ω_0 over 18 days, which include 42 runs made over seven days using five different ion crystals. The normalized χ^2 for these five frequency measurements is 0.77. If we assume that the frequency depends linearly on time, a fit to the data gives a drift of $-5 (9) \times 10^{-16}$/day. Because this is consistent with assumption that the frequency drift is zero, we continue our analysis assuming that the frequency does not drift.

Because we measure the frequency ω_0 with respect to the frequency of the hydrogen maser, we must determine the maser frequency relative to that of the primary standards. This is possible through the mutual reference of International Atomic Time (TAI) [4], letting us determine the average frequency of our Hg$^+$ standard to be $\omega_0 = 2\pi \cdot 40\ 507\ 347\ 996.841\ 59\ (14)\ (41)$ Hz. Here, the first uncertainty is due to the systematic shifts shown in Table 1. The second uncertainty is due to the quoted uncertainty in the frequency of TAI. Our value of ω_0 may be
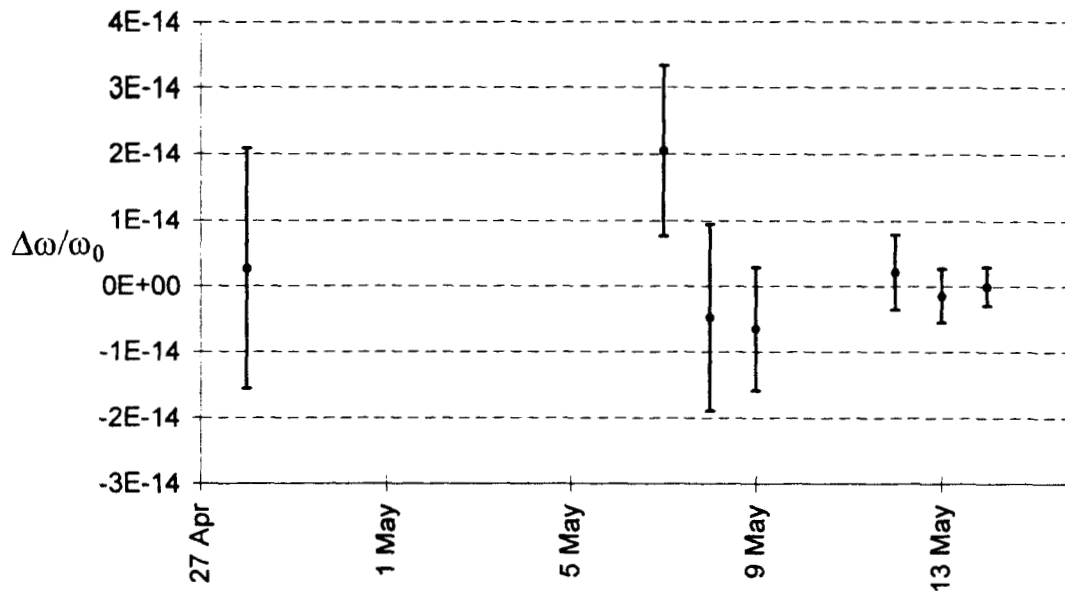
142

Figure 4: Summary of average frequencies over 18 days.

compared with the previous most accurate measurement, which gave $\omega_0/2\pi$ = 40 507 347 996.9 (3) Hz [19]. Our uncertainty from systematic effects (3.4 parts in 10^{15}) is approximately equal to the best values reported, from a cesium beam clock (5 parts in 10^{15}) [20], and a cesium fountain clock (2 parts in 10^{15}) [21].

Our main uncertainties can be greatly reduced in future work. We have built better magnetic shielding to reduce fluctuations in the static magnetic field. The magnetic field at frequency Ω can be reduced by decreasing Ω and the trap dimensions. Use of a smaller trap will also allow linear crystals with more ions, because fringing of the electric fields at the ends of the trap can be reduced and because the radial confinement can be much higher. Finally, by monitoring each ion individually, we can determine their internal states with negligible uncertainty, which will eliminate noise due to laser frequency and intensity fluctuations.

5. Optical Frequency Standard

We are now developing a frequency standard based on the ^{199}Hg$^+$, 282 nm electric quadrupole transition, which has a natural linewidth of 1.7 Hz. Since the clock transition frequency ω_0 is extremely large ($\omega_0/2\pi$ = 1.1 × 10^{15}), the fractional stability can be very high, as seen in Eq. (1). For example, for a single ion probed using the Ramsey technique with a free precession time of 30 ms (limited by the $D_{5/2}$-state lifetime), the fractional
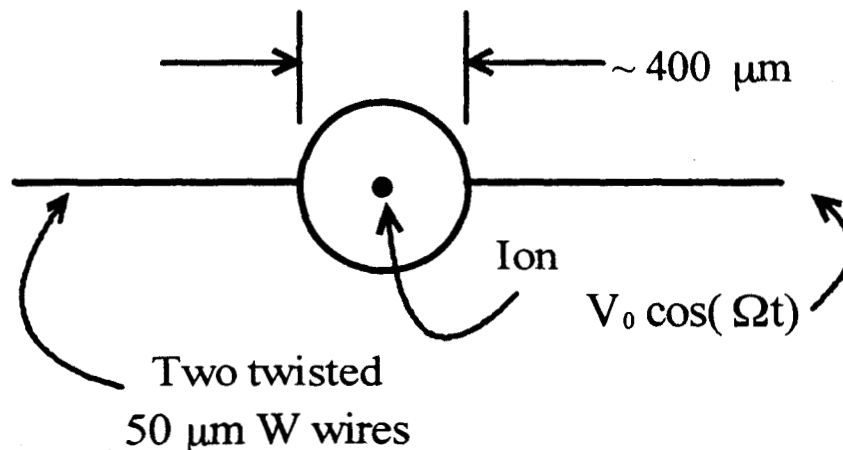

Figure 5: Tight-confining linear Paul trap.

frequency stability is $1 \times 10^{-15} \tau^{-1/2}$, two orders of magnitude better than that of our microwave standard.

Previously at NIST, the frequency of a laser stabilized to about 30 Hz was doubled and then locked to this transition in a single ion confined near the Lamb-Dicke limit [22]. Periodically, the laser frequency was periodically fscanned to obtain a laser-broadened linewidth of approximately 40 Hz at 563 nm [23]. However, the rf trap was in a room temperature environment, where, as explained above, the lifetime of the trapped ion was about ten minutes. To thoroughly investigate such a frequency standard, we require the long observation times provided in the cryogenic environment.

We have built a second cryogenic system that will house a trap for this experiment. We have constructed a Paul-Straubel trap [24] such as that shown schematically in Figure 5. An rf electric potential is applied to the twisted wires, creating the pseudopotential necessary to trap an ion. Although the trapping potential of this trap is weak compared to that of, for example, a linear Paul trap with comparable dimensions, the dimensions of the Paul-Straubel trap can be made very small to compensate for this. Most importantly, the trap can be heated if we run a current through it, removing insulating oxide layers, electrical charge, and patch fields which otherwise leave the trap only very slowly in a cryogenic environment.

6. Narrow-band laser source at 282 nm

To take advantage of the small width of the electric quadrupole transition, the 282 nm source driving the transition must have a linewidth comparable to the width of the atomic resonance. We single-pass 500 mW of 563 nm radiation produced by a dye laser through a 90° phase-matched AD*P crystal to produce up to 100 µW of 282 nm radiation. When the 282 nm light is focused to about 25 µm and there is no Doppler broadening, less than 1 pW will saturate the quadrupole transition.

The frequency of the 563 nm laser is stabilized in two stages [23]. First, the dye laser frequency is stabilized to a cavity with a finesse of about 800 using the Pound-Drever-Hall technique [25]. Low-frequency fluctuations are removed with an intracavity piezo-mounted mirror, while the high-frequency fluctuations are removed by a fast (servo bandwidth > 2 MHz) intracavity electro-optic modulator. This reduces the laser linewidth to about 1 kHz. This stabilized light is transmitted through an optical fiber to a high-finesse cavity. Again, the Pound-Drever-Hall technique is used to lock the frequency of the fiber-transmitted light to the cavity frequency. Low-frequency corrections to the laser frequency, determined by the high-finesse cavities, are fed back to the length of the lower-finesse cavity. Higher-frequency fluctuations are removed with an acousto-optic modulator. This frequency-stabilized light is frequency-doubled and directed toward the trapped ion.

To evaluate the frequency stability of the light, we use two high-finesse cavities, which have been described elsewhere [23]. The spacer of one of the two cavities is made of a 27 cm long, 10 cm diameter Zerodur rod, and that of the second cavity is made of a 10 cm long, 10 cm diameter ULE rod. Both spacers have a hole bored down the rod axis to transmit light. The transmitted power and hence the intracavity power are stabilized to 0.1%. High-reflectance mirrors, whose radii of curvature are chosen so that the modes of the cavities are highly non-degenerate, are optically contacted to the ends of each rod. Each cavity is suspended by two thin W wires inside separate vacuum chambers, whose temperatures are actively stabilized. Each vacuum chamber, much of the optics, and some of the electronics are mounted on separate platforms, which are suspended by several sets of rubber surgical tubing to isolate the cavities from floor and ceiling vibrations. The tilt of each suspended platform is stabilized by servoing the distance of three of its corners from the floor by heating the rubber tubing to adjust its length. The cavity and platform are enclosed in a particle-board box lined with thin layers of lead and foam to reduce acoustical vibrations.

Figure 6 shows a beat note between two laser beams locked to these two independent cavities. The full width at half-maximum of the power spectrum is approximately 8 Hz. If both lasers have the same linewidth, the linewidth of a single laser is about 6 Hz. This is fractionally 1.1 parts in 10^{14} of the laser frequency at 563 nm, which we think is the narrowest recorded linewidth reported.

7. Summary

We have locked the frequency of a synthesizer to the 40.5 GHz transition in laser-cooled strings of ^{199}Hg$^+$ ions in a linear cryogenic rf trap. With a Ramsey period of 100 s and seven ions, the fractional stability of the microwave frequency is $3.2 \times 10^{-13} \tau^{-1/2}$ for measurement times $\tau < 2$ h. We have measured the clock transition frequency with a fractional statistical and systematic uncertainty of 3.4×10^{-15}. This uncertainty is limited primarily by the uncertainty in the Zeeman shift due to fields at the trap frequency Ω, and by fluctuations in the static magnetic
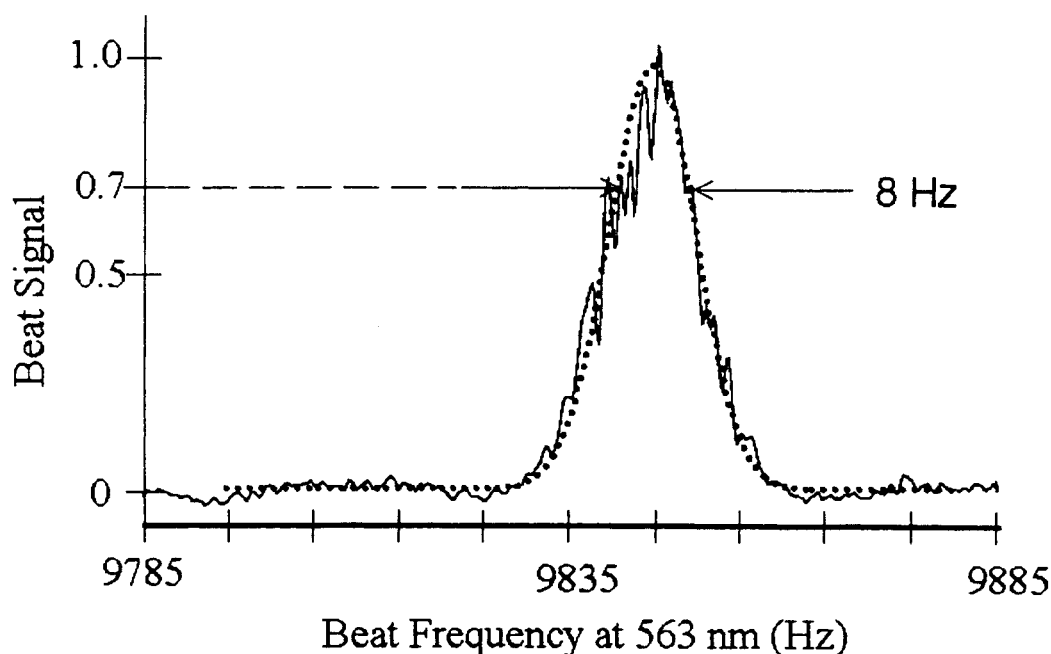
Figure 6:   Beat note between two laser beams locked to independent cavities, integrated over 80 s. The dotted line is a Gaussian line profile meant to guide the eye. The full width at half-maximum of the power spectrum is 8 Hz.

field. We expect that both of these uncertainties will be reduced in future experiments. We are also developing a 282 nm optical frequency standard, whose potential stability is $\sigma_y(\tau) \approx 10^{-15} \tau^{-1/2}$. The lasers used to drive the 282 nm electric quadrupole transition have a frequency stability of less than 10 Hz.

8. Acknowledgments

9. References

*   Work of US Government; not subject to US copyright.

1   R.C. Thompson, "Spectroscopy of Trapped Ions," *Adv. At. Mol. Phys.* **31**, pp. 63-136 (1993), and references therein.

2   J.J. Bollinger, W.M. Itano, D.J. Wineland, and D.J. Heinzen, "Optimal Frequency Measurements with Maximally Correlated States," *Phys. Rev. A* **54**, pp. R4649-4652 (1996).

3   *Proc. 5th Symp. Freq. Standards and Metrology*, ed. J.C. Bergquist (World Scientific, Singapore, 1996).

4   *Proc. IEEE: Special Issue on Time and Freq.* **79** (7), (1991).

5   M.E. Poitzsch, J.C. Bergquist, W.M. Itano, and D. J. Wineland, "Cryogenic Linear Ion Trap for Accurate Spectroscopy," *Rev. Sci. Instrum.* **67**, pp. 129-134 (1996).

6   H.G. Dehmelt, "Introduction to the Session on Trapped Ions," *Proc. 4th Symposium on Freq. Standards and Metrology*, ed. A. Demarchi, p. 286, (Springer Verlag, Heidelberg, 1988).

7   J.D. Prestage, G.J. Dick, and L. Maleki, "New Ion Trap for Frequency Standard Applications," *J. Appl. Phys.* **66**, pp. 1013-1017 (1989).

8   D.J. Wineland, Wayne M. Itano, J.C. Bergquist, J.J. Bollinger, F. Diedrich, and S.L. Gilbert, "High Accuracy Spectroscopy of Stored Ions," *Proc. 4th Symposium on Freq. Standards and Metrology*, ed. A. Demarchi, pp. 71-77 (Springer Verlag, Heidelberg, 1988).

9   W.M. Itano, J.C. Bergquist, J.J. Bollinger, J.M. Gilligan, D.J. Heinzen, F.L. Moore, M.G. Raizen, and D.J. Wineland, "Quantum Projection Noise: Population Fluctuations in Two-level Systems," *Phys. Rev. A* **47**, pp. 3554-3557 (1993).

10 D.J. Berkeland, J.D. Miller, J.C. Bergquist, W.M. Itano, and D.J. Wineland, "Minimization of Ion Micromotion in a Paul Trap," submitted for publication in *J. Appl. Phys.*, November, 1997.

11 M.G. Raizen, J.M. Gilligan, J.C. Bergquist, W.M. Itano, and D.J. Wineland, "Ionic Crystals in a Linear Paul Trap," *Phys. Rev. A* **45**, pp. 6493-6501 (1992).

12 W.M. Itano, L.L. Lewis, and D.J. Wineland, "Shift of $^2S_{1/2}$ Hyperfine Splittings Due to Blackbody Radiation," *Phys. Rev. A* **25**, pp. 1233-1235 (1982).

13 D.J. Berkeland, F.C. Cruz and J.C. Bergquist, "Sum-frequency Generation of Continuous-wave Light at 194 nm," *Appl. Opt.* **2006**, pp. 4159-4162 (1997).

14 N.F. Ramsey, *Molecular Beams*, pp. 124-134 (Oxford Univ. Press, London, 1956).

15 C.W. Nelson, F.L. Walls, F.G. Ascarrunz, and P.A. Pond, "Progress on Prototype Synthesizer Electronics for $^{199}Hg^+$ at 40.5 GHz," *Proc. 1992 IEEE Freq. Control Symp.*, pp. 64-68 (1992).

16 W.D. Lee, J.H. Shirley, J.P. Lowe, and R.E. Drullinger, "The Accuracy Evaluation of NIST-7," *IEEE Trans. Instrum. Meas.* **44**, pp. 120-123 (1995).

17 A. Clairon, S. Ghezali, G. Santarelli, Ph. Laurent, S.N. Lea, M. Bahoura, E. Simon, S. Weyers, and K. Szymaniec, "Preliminary Accuracy Evaluation of a Cesium Fountain Frequency Standard," in Ref. 3, pp. 49-59.

18 D.J. Berkeland, J.D. Miller, J.C. Bergquist, W.M. Itano, and D.J. Wineland, "Laser-Cooled Mercury Ion Frequency Standard," to be published in *Phys. Rev. Lett.*.

19 L.S. Cutler, R.P. Giffard, and M.D. McGuire, "A Trapped Mercury 199 Ion Frequency Standard," *Proc. 13th Ann. PTTI Appl. And Planning Meeting*, NASA Conf. Publ. 2220, pp. 563-578 (1981).

20 R.E. Drullinger, J.H. Shirley and W.D. Lee, "NIST-7, the U.S. Primary Frequency Standard: New Evaluation Techniques," *28th Ann. PTTI Appl. And Planning Mtg.*, pp. 255-264 (1996).

21 E. Simon, P. Laurent, C. Mandache and A. Clairon, "Experimental Measurement of the Shift of Cs Hyperfine Splittings Due to a Static Electric Field," *11th Eur. Freq. And Time Forum Neuchatel*, pp. 43-45 (1997).

22 R.H. Dicke, "The Effect of Collisions upon the Doppler Width of Spectral Lines," *Phys. Rev.* **89**, pp. 472-473 (1953).

23 J.C. Bergquist, W.M. Itano, and D.J. Wineland, "Laser Stabilization to a Single Ion," in *Frontiers in Laser Spectroscopy*, pp. 359-376 (1994).

24 Nan Yu, W. Nagourney, and H. Dehmelt, "Demonstration of a New Paul-Straubel Trap for Trapping Single Ions," *J. Appl. Phys.* **69**, pp. 3779-3781 (1991).

25 R.W. P. Drever, J.L. Hall, F.V. Kowalski, J. Hough, G.M. Ford, A.J. Munley, and H. Ward, "Laser Phase and Frequency Stabilization Using an Optical Resonator," *Appl. Phys. B* **31**, pp. 97-105 (1983).